INTERNATIONAL SYMPOSIUM: WAVES – PHYSICAL AND NUMERICAL MODELLING

UNIVERSITY OF BRITISH COLUMBIA, VANCOUVER, CANADA

AUGUST 21 - 24, 1994

DEVELOPMENT OF A THIRD-GENERATION OCEAN WAVE MODEL AT NOAA/NMC. [1]

H.L. Tolman and D.V. Chalikov
UCAR visiting scientists, Marine Prediction Branch
Development Division, NOAA/NMC21
5200 Auth Road, Camp Springs, MD 20746, USA

ABSTRACT

A new third generation wave model (WAVEWATCH III) is presently being developed at NOAA/NMC. The present paper gives a general description of the model and focusses on (i) the functional design, (ii) the governing balance equation and a new variable-grid approach developed for this equation, and (iii) on the development of a new source term package. The new source terms are shown to improve fetch-limited model behavior significantly. Our approach to dissipation, considering high and low frequency dissipation separately, potentially simplifies the systematic investigation of the effects of whitecapping within the wave energy balance.

INTRODUCTION

Wave prediction has been an integral part of the activities of the Marine Prediction Branch of the Development Division of NOAA/NMC for several years. Until recently, all forecasts were made using a locally customized implementation of the second-generation SAIL model [Greenwood et al., 1985)], the so-called NOW (NOAA Operational Wave) model. More recently, several versions of the third generation WAM model [WAMDIG (1988)] have been implemented. A third-generation wave model integrates the spectral energy balance equation using first principles only, i.e., without assuming a spectral

[1] OPC contribution Nr. 88.

shape. Such models are significantly more expensive than previous models, but are generally assumed to be superior as they (by design) are universally applicable without the need of re-tuning, and as they allow for direct implementation of new parameterizations of the actual physical processes.

In spite of the apparent success of the WAM model, there is room for improvement in third generation wave modelling. WAM uses simple first order propagation schemes, and the source terms of WAM result in inaccurate growth behavior for short fetches (as will be shown below). Optimization considerations have furthermore influenced the transparency of the source code of WAM, which somewhat hampers experiments to improve WAM. Considering the above, development of a new third-generation wave model has been initiated at NOAA/NMC. This model (WAVEWATCH III) is a further development of WAM and WAVEWATCH (Tolman, 1991). Its application is intended for global and regional scales, with grid resolutions of typically 10 km or larger, and depths of typically 10 m and larger.

Presently (march 1994), the general system design for WAVEWATCH III has been finished, and a test version of the new model using simple first order propagation schemes and the source terms of WAM cycles 1-3 has been coded, tested and optimized. Meanwhile, a new source term package is being developed independently (using WAVEWATCH II, Tolman 1991, 1992). The search for a new propagation schemes is still ongoing, although several proven higher order scheme are readily available [e.g., Neu and Won (1990), Tolman (1991, 1992)]. As the model is still under development, a complete description cannot be given here. The present paper will consider the following subjects. First, the functional design of the model will be discussed briefly, together with the computational economy of the model. Secondly, the selected balance equation will be discussed, together with a new variable-grid approach used to solve this equation. Thirdly we will outline the new physics package and present some initial results for standard fetch-limited wave growth tests.

MODEL DESIGN

The intended range of application of the new model as described above implies that effects of finite depths and currents are potentially important. The bathymetric scales, however, are generally much larger than the scale of individual waves. Diffraction is therefore ignored and depths and currents are assumed to vary slowly compared to the scales of a single wave. The corresponding balance equation will be discussed in the following section. The intended applications dictate functional requirements such as (i) accounting for dynamically adjusted ice coverage, (ii) data transfer between nested implementations, (iii) full plug compatibility and (iv) a transparent code. The latter two requirements are desirable to simplify experiments with new source term parameterizations and new numerical approaches, and to facilitate later inclusion in larger model systems (coupled models and data assimilation).

To assure maximum transparency, propagation and source terms are numerically

decoupled, as are propagation in physical and spectral space. This splitting technique leaves sufficient options for vectorization and strongly promotes parallelization. This is illustrated in Table 1, in which the CPU and wallclock times of a global implementation of the test version of WAVEWATCH III and the semi-operational global implementation of WAM at NOAA/NMC are compared. Both models use a $2.5° \times 2.5°$ longitude-latitude resolution with 5655 sea points and 25 discrete spectral frequencies. WAVEWATCH III uses 24 directions and WAM uses 12 directions. Although WAVEWATCH III thus incorporates twice the number of degrees of freedom compared to WAM, it proved only slightly more expensive, and is efficiently parallelized (see Table 1).

Two remarks need to be made on the comparison in Table 1. First, we compare WAM cycle 4 with a model including the physics of WAM cycle 3. The upgrading of WAM from cycle 3 to cycle 4 increases computation effort by approximately 10%. Secondly, a significant part of the gain in efficiency of WAVEWATCH III over WAM is due to the fact that the dynamic source term integration scheme of WAVEWATCH III (as described below) increases the effective source term time step from 20 min. in WAM to approximately 27 min. in WAVEWATCH III. This gain is possible because of the propagation time step of 40 min used for this spatial resolution. For higher spatial resolutions time steps in both models will be dictated by the CFL criterion, in which case the CPU time required for WAVEWATCH III will be closer to that of WAM.

THE BALANCE EQUATION

Wind waves on slowly varying depths (d) and currents ($\mathbf{U}$) are most elegantly described with a spectral action balance equation (e.g., Bretherthon and Garrett, 1968; Whitham, 1974). In the linear approach the action spectrum is two-dimensional and can be described as a function the spectral direction θ and either the wavenumber k, the relative or intrinsic frequency σ (as observed when moving with $\mathbf{U}$) or the absolute frequency ω (as observed in a fixed frame of reference). For slowly varying currents, the latter three 'phase' parameters are interrelated through the dispersion relation and a Doppler equation.

$$\sigma^2 = gk \tanh kd \,, \tag{1}$$

$$\omega = \sigma + \mathbf{k} \cdot \mathbf{U} \,. \tag{2}$$

Traditionally, wind waves are described with the variance spectrum as a function of the frequency $f = \omega/2\pi$ and the direction θ, $F(f,\theta)$, or the corresponding wave action spectrum $N(f,\theta) = F(f,\theta)/\sigma$. From a theoretical point of view, however, the wavenumber spectrum $N(k,\theta)$ has been considered more appropriate for modeling wind waves due to its invariance properties with respect to the water depth for the physics of wave growth and decay (e.g., Kitaigorodskii, 1962, 1983; Kitaigorodskii et al., 1975; Bouws et al., 1985). The governing equations for the evolution of this spectrum can

be written as (e.g., Hasselmann et al., 1973; Willebrand, 1974)

$$\frac{\partial N}{\partial t} + \nabla_x \cdot \dot{\mathbf{x}} N + \frac{\partial}{\partial \theta}\dot{\theta} N + \frac{\partial}{\partial k}\dot{k} N = \frac{S}{\sigma} \,, \tag{3}$$

$$\dot{\mathbf{x}} = \mathbf{c}_g + \mathbf{U} \,, \tag{4}$$

$$\dot{\theta} = -\frac{1}{k}\left[\frac{\partial \sigma}{\partial d}\frac{\partial d}{\partial m} - \mathbf{k} \cdot \frac{\partial \mathbf{U}}{\partial m}\right] \,, \tag{5}$$

$$\dot{k} = -\frac{\partial \sigma}{\partial d}\frac{\partial d}{\partial s} - \mathbf{k} \cdot \frac{\partial \mathbf{U}}{\partial s} \,, \tag{6}$$

where the group velocity $\mathbf{c}_g$ is given by $c_g \equiv \partial\sigma/\partial k$ and θ, s is a coordinate in the direction θ, m is a coordinate perpendicular to s and S represents the net source term for wave generation and dissipation. For convenience of notation, the dependency of N and S on k and θ has been neglected.

The use of these equations for the wavenumber spectrum has a (numerical) disadvantage for waves propagating from deep to shallow water. In such conditions, long waves are significantly shortened (i.e., k increases significantly), as is illustrated in Fig. 1. If the k-space of the spectrum is discretized with an invariant wavenumber grid, as is common practice in wave models, this leads to a loss of resolution in shallow water. However, this 'shoaling' is a reversible process, which suggest that its effects can be incorporated in a variable wavenumber grid. The potential of such a grid to eliminate numerical disadvantages for limited depths and mean currents will be discussed in detail elsewhere. In WAVEWATCH III a spatially and temporally invariant σ-grid is used. The corresponding wavenumber grid is a function of the instantaneous depth only (see Fig. 1). Transformed to this grid, the governing equations (3) and (6) become

$$\frac{\partial N}{\partial t} + c_g \nabla_x \cdot \left(\frac{\dot{\mathbf{x}} N}{c_g}\right) + \frac{\partial}{\partial \theta}\dot{\theta} N + \frac{\partial}{\partial k}\dot{k}_g N = \frac{S}{\sigma} + c_g^{-1}\frac{\partial \sigma}{\partial d}\frac{\partial d}{\partial t}\frac{\partial N}{\partial k} \,, \tag{7}$$

$$\dot{k}_g = \frac{\mathbf{U} \cdot \nabla_x d}{c_g}\frac{\partial \sigma}{\partial d} - \mathbf{k} \cdot \frac{\partial \mathbf{U}}{\partial s} \,. \tag{8}$$

whereas Eqs. (4) and (5) remain unchanged. The equation for the variable grid differs from the original balance equation (3) on three points.

First, an additional term arises at the right side of the equation. This term represents a change of grid due to temporal variations of the depth, without changing the actual spectrum $N(k,\theta)$. The numerically non-conservative nature of this term is potentially disadvantageous. However, it can be shown that this term is generally small, and that water levels can generally be updated sparsely. Without loss of generality, the corresponding part of Eq. (7) can then be replaced with a conservative interpolation between the new and the old grid. The remaining balance equation is quasi-steady with respect to the depth.

Secondly, the term describing propagation in physical space [second term in Eq. (3)] is modified to account for the spatially varying 'band width' in the k-grid. For quasi-steady depths, the propagation equation can be re-written as

$$\frac{\partial \mathcal{N}}{\partial t} + \nabla_x \cdot \dot{\mathbf{x}} \mathcal{N} + \frac{\partial}{\partial \theta} \dot{\theta} \mathcal{N} + \frac{\partial}{\partial k} \dot{k}_g \mathcal{N} = 0 \,, \tag{9}$$

where $\mathcal{N} = N c_g^{-1}$ becomes the propagated quantity. This result in not surprising, as $\mathcal{N}$ in represents the frequency-direction spectrum $\mathcal{N}(\sigma, \theta)$, for which Eq. (9) is the propagation equation.

Finally, the propagation velocity in k-space is modified to represent the propagation velocity relative to the grid ($\dot{k}_g$). In cases without currents, this propagation velocity becomes zero, which implies that all effects of shoaling are included in the grid. Effects of mean currents are not incorporated in the grid, and hence remain a part of the propagation equation. Note that the first term on the right side of Eq. (8) represents an effect of mean currents on shoaling.

The discussion of Eq. (9) indicates that the present approach can be interpreted as a hybrid method considering both wavenumber and frequency spectra. Its particular advantage is that it gives a elegant and consistent way to deal with temporal variations of the water depth, by sparsely updating water levels. The present approach is furthermore hybrid in the sense that effects of depth variations are included in the grid, whereas effects of currents remain an explicitly part of the balance equation.

SOURCE TERMS

The present test version of WAVEWATCH III includes the source terms of WAM cycles 1 through 3, i.e., an input source term based on Snyder et al. (1981), nonlinear interactions according to Hasselmann et al. (1985) and the whitecapping source term of Komen et al. (1984) (see also WAMDIG, 1988). Due to the above time splitting, the source term step effectively becomes a point model, which is applied to each spatial grid point separately. This allows for a simple plug-compatible structure in which source terms are easily interchanged, and for a 'dynamic' integration scheme, where the time step for integration is determined independently for each spatial grid point (Tolman, 1992). The 'dynamic' time step Δt_d depends on the net source term S/σ, and on a maximum allowed change of action density ΔN_m,

$$\Delta t_d^n = \min_{f<f_c} \left[\frac{\Delta N_m}{|S/\sigma|} \left(1 + 0.5 D \frac{\Delta N_m}{|S/\sigma|} \right)^{-1} \right] , \tag{10}$$

and is limited for the integration time not to exceed the overall propagation time step Δt, and not to become excessively small. Here f_c is the cut-off frequency between the diagnostic and prognostic parts of the spectrum, and D is the diagonal contribution

of the derivative of S/σ with respect to N (both defined as in WAM). Integration over Δt_d results in a new action density

$$N = \max \left(0 \,,\, N + \frac{S \Delta t_d}{\sigma (1 - 0.5 D \Delta t_d)} \right) . \tag{11}$$

The maximum change of action density ΔN_m is determined as the minimum of a parametric change (defined as a fraction of the Pierson-Moskowitz equilibrium level), and a filtered relative change (equations not presented here). The advantage of this scheme is that it concentrates computational effort in regions where this is required, i.e., in regions with rapidly changing wind or wave conditions (see Tolman 1992, Fig. 5). Simultaneously, it can increase integration time steps and decrease the computational effort in areas with low wind speeds and/or fairly steady wave conditions. The latter can increase the effective time step for source term integration well beyond the fixed 20 min. time step for source term integration of WAM, provided that the propagation time step $\Delta t > 20$ min.

The classical source terms of WAM result in a significant overestimation of wave growth for short fetches. This is illustrated in Fig. 2, which shows a systematic overestimation of the wave energy $E = \int\int F(f, \theta)\, df\, d\theta$ and a corresponding underestimation of the peak frequency f_p for short fetches when compared to the JONSWAP data. Note that this behavior is somewhat worse than that of the actual WAM model, as the dynamic integration method effectively boosts growth for small fetches. Hence WAM shows slightly better results due to partial cancellation of numerical and physical errors.

New source term parameterizations for WAVEWATCH III are presently developed independently using WAVEWATCH II (Tolman 1991, 1992). We adopted the input source term of Chalikov and Belevich (1993), which is based on numerical simulation of the statistical structure of air flow over irregular waves using Reynolds' equations. It differs from the input source term of Snyder et al. (1981) on three main points. (i) It allows for energy transfer from waves to wind for waves whose apparent phase velocity $c/\cos(\theta - \theta_{wind})$ is larger than the wind speed. (ii) It results in a 2 to 3 times smaller integral energy input. (iii) Growth rates for high-frequency waves depend quadratically on the wind speed, and can become much larger than predicted by Snyder et al. We furthermore adopted the parameterization of Hasselmann et al. (1985) to estimate nonlinear interactions, as this is presently the only economically feasible parameterization for operational wave models. Finally, we are developing new parameterizations for the dissipation source term. In this we recognize that the dissipation in the high-frequency equilibrium range of the spectrum has to be fundamentally different from dissipation for the spectral peak and lower frequencies. The 'low frequency' dissipation has to be quasi-linear in terms of spectral densities, because small differences in the spectral shape for frequencies near or below the spectral peak frequency cannot be expected to have a significant impact on the integral energy dissipation. The actual magnitude of the dissipation then depends mainly on mean wave parameters. In the equilibrium

range of the spectrum, however, the source terms are expected to be in a local quasi-steady balance, suggesting that the magnitude of the dissipation mainly depends on spectral properties in a limited frequency range. As the equilibrium range of the spectrum is fairly independent of the fetch, the high-frequency dissipation is expected to be a weak function of mean wave parameters at best. In our numerical experiments we assume that the low-frequency dissipation source term can be described as turbulent dissipation

$$S_{turb} = -2\Phi\, u_* \, h_w \, k^2 \, F(k,\theta)\,, \qquad (12)$$

where u_* is the friction velocity, h_w is a length scale related to the wave energy in the high-frequency range of the spectrum, and where Φ is an empirical function of the nondimensional energy or the non-dimensional frequency. For the high-frequency dissipation term we have been experimenting with several diagnostic and explicit formulations.

In Fig 3 preliminary results are presented as obtained with a diagnostic high-frequency dissipation source term, in which the high-frequency part of the spectrum is artificially relaxed to an f^{-4} shape. These preliminary results indicate the potential of the present approach to significantly improve the behavior of the model short fetches. Recent experiments indicate, that the above improvement can also be obtained with explicit formulations for the high-frequency dissipation. Note that the excellent model representation of the wave energy E might have been expected, as Φ in Eq. (12) effectively is tuned as a function of fetch, because both the nondimensional energy and frequency are exclusive functions of the fetch. However, this does not imply that the model has to result in realistic spectra or sufficient wave growth. In fact, one might have expected the input source term of Chalikov and Belevich to be too weak to result in realistic wave growth. Note that peak frequency data was not used in tuning the model. The significant improvement of the behavior of f_p therefore indicates that the new source terms result in fairly realistic spectra.

CONCLUDING REMARKS

In the present paper we have presented some features of a new third-generation wave model. This model features a variable grid approach to eliminate implicit numerical disadvantages of modeling the development of wavenumber spectra. It will furthermore features new source term parameterizations, which significantly improve short-fetch model behavior. In particular the dissipation source term, however, is not well rooted in theory, and should still be considered as a first crude approximation used to close the energy balance equation. Perhaps more important than the improved model behavior is the realization that dissipation at high and low frequencies should be treated differently. This implies that the low-frequency dissipation source term is no longer required to produce a realistic balance at high frequencies, where this source term is not likely to

be valid. We hope that this will simplify future investigations into the spectral nature of whitecapping dissipation.

REFERENCES

Bouws, E. and H. Günter, W. Rosenthal and C.L. Vincent, 1985: Similarity of the wind wave spectrum in finite depth water. 1: Spectral form. *J. Geophys. Res.*, **90**, 975-986.

Bretherthon, F.P., and C.J.R. Garrett, 1968: Wave trains in inhomogeneous moving media. *Proc. Roy. Soc. London*, **A 302**, 529-554.

Chalikov, D.V. and M.Yu. Belevich, 1993: One-dimensional theory of the wave boundary layer. *Bound.-Layer Met.*, **63**, 65-96.

Hasselmann, K., T.P. Barnett, E. Bouws, H. Carlson, D.E. Cartwright, K. Enke, J.A. Ewing, H. Gienapp, D.E. Hasselmann, P. Kruseman, A. Meerburg, P. Müller, D.J. Olbers, K. Richter, W. Sell and H. Walden, 1973: Measurements of wind-wave growth and swell decay during the Joint North Sea Wave Project (JONSWAP). *Ergänzungsheft zur Deutschen Hydrographischen Zeitschrift*, Reihe A (8) Nr. 12, 95 pp.

Hasselmann, S., K. Hasselmann, J.H. Allender and T.P. Barnett, 1985: Computations and parameterizations of the nonlinear energy transfer in a gravity-wave spectrum. Part II: Parameterizations of the nonlinear energy transfer for application in wave models. *J. Phys. Oceanogr.*, **15**, 1378-1391.

Kitaigorodskii, S.A., 1962: Application of the theory of similarity to the analysis of wind-generated wave motion as a stochastic process. *Bull. Acad. Sci. USSR Geophys. Ser. 1*, **73**, 105-117.

——, 1983: On the theory of the equilibrium range in the spectrum of wind-generated gravity waves. *J. Phys. Oceanogr.*, **18**, 816-827.

——, V.P. Krasitskii and M.M. Zaslavskii, 1975: On Phillips theory of equilibrium range in the spectra of wind-generated gravity waves. *J. Phys. Oceanogr.*, **5**, 410-420.

Komen, G.J., S. Hasselmann and K. Hasselmann, 1984: On the existence of a fully developed wind-sea spectrum. *J. Phys. Oceanogr.*, **14**, 1271-1285.

Neu, W.L. and Y.S. Won 1990: Propagation schemes for wind wave models with finite depth and current. *Ocean wave mechanics, computational fluid dynamics and mathematical modeling*, M. Rahman Ed., Computational Mechanics Publications, 947-954

Tolman, H.L., 1991: A third-generation model for wind waves on slowly varying, unsteady and inhomogeneous depths and currents. *J. Phys. Oceanogr.*, **21**, 782-797.

——, 1992: Effects of numerics on the physics in a third-generation wind-wave model. *J. Phys. Oceanogr.*, **22**, 1095-1111.

WAMDIG, 1988: The WAM model - a third generation ocean wave prediction model. *J. Phys. Oceanogr.*, **18**, 1775-1810.

Snyder, R.L., F.W. Dobson , J.A. Elliott and R.B. Long, 1981: Array measurements of atmospheric pressure fluctuations above surface gravity waves. *J. Fluid Mech.*, **102**, 1-59.

Whitham, G.B., 1974: *Linear and nonlinear waves*, Wiley, New York, 636 pp.

Willebrand, J., 1974: Energy transport in a nonlinear and inhomogeneous random gravity wave field. *J. Fluid Mech.*, **70**, 113-126.

Table 1 Run time comparison between WAM and WAVEWATCH III for a global 2.5° × 2.5° implementation with 25 spectral frequencies and 12 (WAM) or 24 (WAVEWATCH III) spectral directions on a CRAY Y-MP with 8 CPUs. Results for 1 CPU represent actual CPU times, results for multiple CPU runs represent wall-clock times, which represent a conservative estimate from low-priority batch jobs.

	WAM cycle 4	WAVEWATCH III (WAM cycle 3 physics)		
	1 CPU	1 CPU	2 CPUs	4 CPUs
elapsed time for 1 day hindcast (s)	220	290	150	90
avg. number of CPUs connected	1	1	1.96	3.68

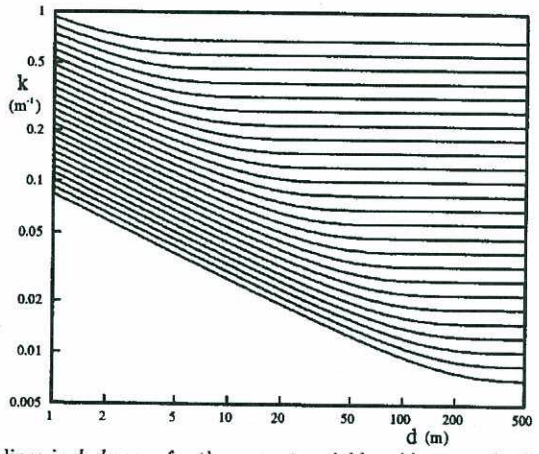

Fig. 1 Grid lines in k-d space for the present variable grid approach. In deep water, the grid corresponds to the common WAM grid with 25 frequencies, $f_{i+1} = 1.1 f_i$ and $f_1 = 0.0418$ Hz. The grid lines correspond to characteristics for steady water depths.

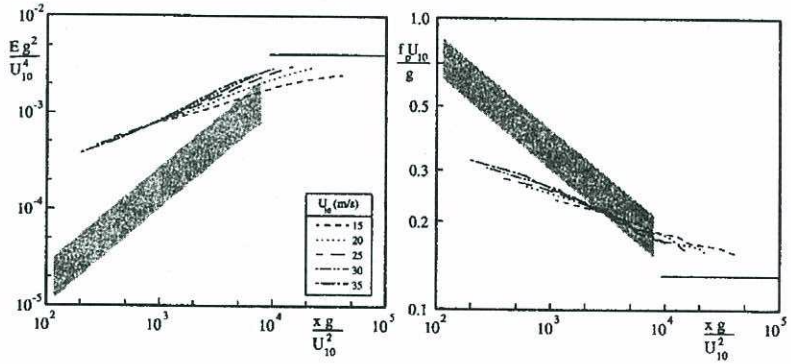

Fig. 2 The nondimensional energy Eg^2/U_{10}^4 (left panel) and the nondimensional peak frequency $f_p U_{10}/g$ (right panel) as a function of the nondimensional fetch xg/U_{10}^2 for the source terms of WAM cycle 3 and several wind speeds U_{10}. $\Delta x = 25$ km, 38 sea points, $\Delta t = 15$ min. The shaded area represents the JONSWAP data. The solid line represents full-grown (Pierson-Moskowitz) conditions.

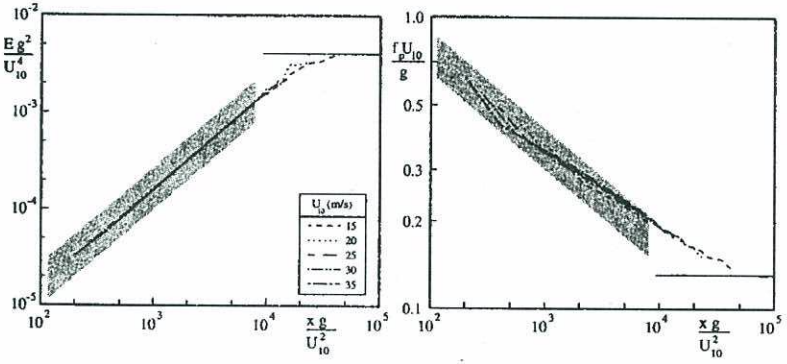

Fig. 3 Like Fig. 2 for the new source terms.